Chapter 9

Investigating EM Dipole Radiating Element for Dual Polarized Phased Array Weather Radars

Ridhwan Khalid Mirza, Yan (Rockee) Zhang,
Dusan Zrnic and Richard Doviak

Additional information is available at the end of the chapter

http://dx.doi.org/10.5772/66502

Abstract

Dual-polarized antenna radiating element is a critical component in the Multi-function Phased Array Radar (MPAR). This paper studies the dual-polarized radiating element based on the EM dipole concept. Two different geometries, i.e., loop approximated as magnetic dipole and a printed electric dipole, are used to form a single dual-polarized radiating element. Radiation patterns based on Ansoft HFSS (High Frequency Structural Simulator) simulation software and measurements carried out in anechoic chambers are presented. Initial array design based on these elements will also be discussed.

Keywords: MPAR, dual-polarized elements, cross pol, E&M dipole array, loop antenna, electric dipole

1. Introduction

Multi-function Phased Array Radars (MPARs) are being considered for fulfilling the need of FAA, NOAA/NWS, and possibly Homeland security [1]. One of the specific goals of deploying MPAR systems is to replace the current Weather Surveillance Radar (WSR-88D radar) and other air-traffic control radars as upgrade [2]. In many radar applications and weather radar polarimetry, the physical symmetry of the target and weather scan moments can be detected by phased array antennas which require suppression of antenna cross polarization (X-pol) especially during the main beam shift or scanning off-broadside direction [3, 4]. Dual-polarized antenna radiating element plays a key role in such systems. The current state-of-the-art parabolic reflector antennas which are used for weather surveillance are required to scan mechanically and lack the ability to scan the beam electronically in contrast

to phased array radars. The cross polarization (X-pol) isolation of phased array radar can be improved effectively if the cross polarization levels of individual antenna radiating elements are minimized.

Orthogonally signals can be transmitted or received without extra bandwidth requirement or physical separation between antennas through a dual-polarized radiating element, which enables observing backscattering from targets (precipitation, clutter, etc.) from horizontally and vertically polarized electromagnetic waves. For instance, vertical tree trunks and structures can be tracked by HH polarization. VV polarization can provide water and soil scattering information [5]. However, for accurate polar metric measurements, it is required for the antenna to have high cross polarization suppression. The cross polarization isolation as required by many weather polarimetry applications is less than 20 dB for alternate transmission and less than 40 dB for simultaneous transmission and reception [2, 6].

There are many other forms of antennas in the form of microstrip patches which are used widely in Multi-Functional Phased Array Radars (MPARs) [4, 7, 8]. Although better than -30 dB cross pol levels are achieved in most of the rectangular patch-based MPAR subarray prototypes, however, there are certain challenges which arise when steered-beam calibrations are needed for precise dual-pol measurements. The main challenge arises when scanning the beam off-broadside direction, and the relationship between co-pol and cross pol electric fields is not consistent for different pointing angles of an antenna [8]. An ideal radiating element should be able to radiate electric fields which are orthogonal to each other for two different polarizations [2, 9]. To achieve this, two types of dual polarization elements are considered. The first one is a pair of cross dipole or orthogonal dipole element configuration in which the electric fields are orthogonal only in principal planes which is under investigation by many researchers [10–12]. The other type of radiator is a pair of magnetic dipole and electric dipole for which the electric fields are orthogonal in all spatial directions. The latter configuration is investigated and proposed in this book chapter as the dual-polarized radiating element.

If these types of elements which have orthogonal electric fields are used, especially for cylindrical phased array radars (CPARs), the problems of surface and traveling waves can be effectively avoided [8]. Presently, the main disadvantages of using the dipole elements are higher costs for fabrication and potential requirements of three-dimensional structures. However, these disadvantages outweigh the potential benefits of using such a configuration especially for polarimetric phased array radars which have strict constraint of maintaining orthogonality between two different polarizations.

This chapter/proposal studies different antenna geometries such as loop and planar dipoles. The characteristics of these radiating element designs are evaluated with HFSS simulations. The simulations show that these structures result in unidirectional circular current distribution; improvement at all aspects of the antenna characteristics including radiation pattern, return loss, and cross polarization isolations at single element level will be discussed. The far-field radiation patterns for the radiating elements will be displayed as measured in anechoic chambers at Radar Innovations Lab, University of Oklahoma.

http://dx.doi.org/10.5772/66502

2. Background

This section describes the basic theory on the electromagnetic fields, antenna coordinate system, and basic definitions used in this chapter.

2.1. Electromagnetic field regions around an antenna

The antenna radiates waves in the form of electromagnetic radiation. Hence, defining the field regions around an antenna is lucrative to know, and this will be used for the later in the chapter while discussing results and radiation patterns. The space surrounding any antenna is divided into three regions based on the distance from the antenna under test (AUT). These regions are based on equations as described **Table 1** [9].

Table 1 shows three different regions around an antenna based on the distance. These are calculated based on the equations where r is the distance from the source or AUT, D is the maximum dimension of the AUT, and λ is the wavelength of the radiation. The field region of antenna will be helpful to study and analyze the antenna radiation patterns discussed later in the chapter. Most of the times, the targets are placed or objects are measured in the far-field or Fraunhofer region. These regions are also illustrated in **Figure 1**.

2.2. Antenna coordinate system

The radiation characteristics of an antenna are analyzed using a coordinate system. There are different types like cylindrical, planar, and spherical. However since the antenna for the phased array is to be used in the far field, the spherical coordinate system is optimal as shown in **Figure 2**. In this system the antenna is placed at the origin and r is the distance or radius from the AUT to the observation point. The radiation characteristics of an AUT are determined by varying the elevation or zenith angle θ and azimuth angle ϕ, and field vectors E_θ, E_ϕ are calculated. This spherical coordinate system is used in this chapter for simulation and carrying out measurements in the anechoic chambers.

Region	Distance
Near-field or reactive near-field region	$0 < r < 0.62\sqrt{\frac{D^3}{\lambda}}$
Reactive near-field or Fresnel region	$0.62\sqrt{\frac{D^3}{\lambda}} \leq r \leq 2\frac{D^2}{\lambda}$
Far-field or Fraunhofer region	$2\frac{D^2}{\lambda} \leq r$

Table 1. Field regions around an antenna.

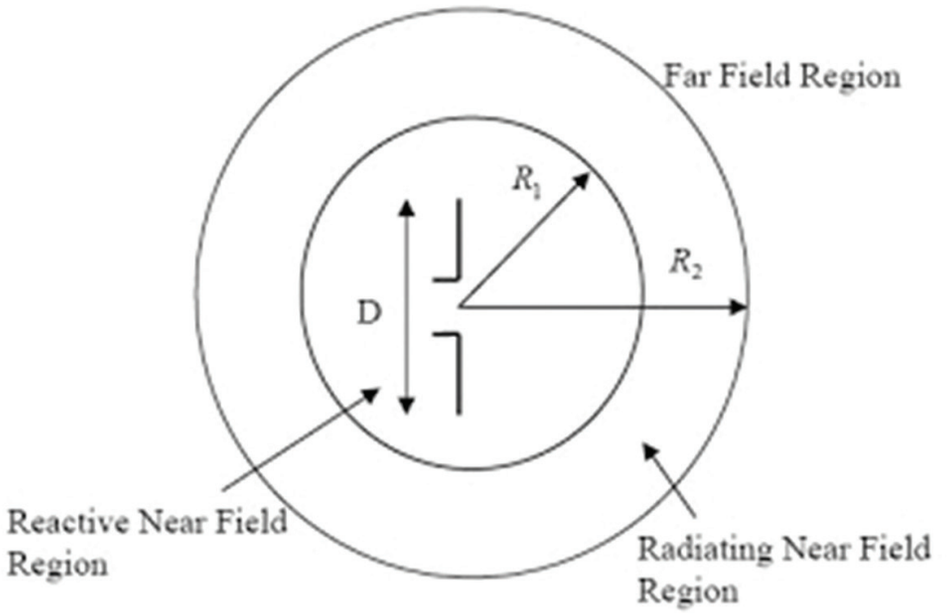

Figure 1. Field regions around an antenna.

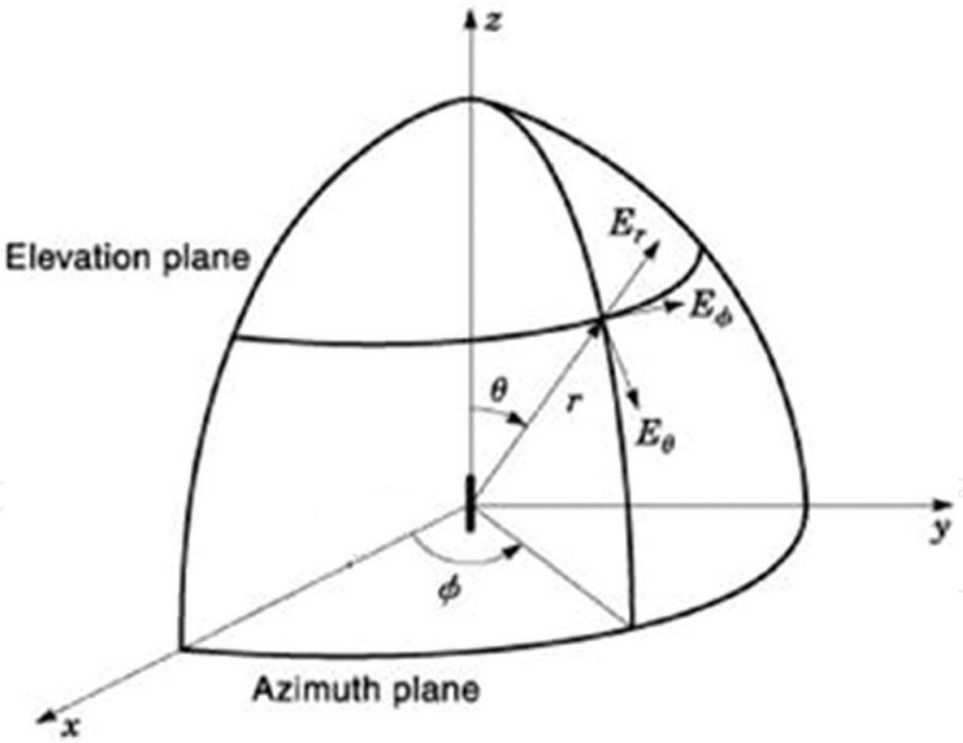

Figure 2. Spherical coordinate system used for antenna analysis [9].

2.3. Antenna polarizations

The polarization of the radiated electric fields produced by an antenna in a given direction is referred as polarization of an antenna. The polarizations of antenna depend on the way the antenna radiates waves and can be studied in open literature [9].

http://dx.doi.org/10.5772/66502

In weather radar polarimetry, there are two important polarization definitions: copolarization (often called as co-pol) and cross polarization (often called as cross pol or X-pol) of a radiating element. The term copolarization is the desired polarization component of the radiation pattern, and cross polarization is the unwanted component of radiation pattern. For instance, if the transmitting antenna is meant to transmit horizontally polarized waves and the receiving antenna on the other end is receiving horizontally polarized waves, it is said to receive co-pol radiation or desired radiation. On the contrary if the receiving antenna was supposed to receive vertically polarized waves, it is receiving cross polarization or unwanted radiation.

There are three most widely used definitions for cross pol and co-pol as given by Ludwig [13]. For weather radars, the second definition of Ludwig (L2) is widely accepted to define the co- and cross polarizations (**Figure 3**).

According to Ludwig's second definition [13], we have

$$\hat{\imath}_{ref} = \frac{sin\phi cos\theta\ \hat{\imath}_{\theta} + cos\phi\,\hat{\imath}_{\phi}}{\sqrt{1 - sin^2\theta sin^2\phi}} \tag{1}$$

$$\hat{\imath}_{cross} = \frac{cos\phi\,\hat{\imath}_{\theta} - cos\theta sin\phi\,\hat{\imath}_{\phi}}{\sqrt{1 - sin^2\theta sin^2\phi}} \tag{2}$$

where $\hat{\imath}_{ref}$ and $\hat{\imath}_{cross}$ are the projections of electric field vectors onto spherical unit vectors given by Ludwig [13] such that,

$E \cdot \hat{\imath}_{ref}$ = the reference polarization (co-pol) component of E

$E \cdot \hat{\imath}_{cross}$ = the cross polarization (cross pol) component of E

The spherical coordinate system used for the weather radar polarimetry and most of the standard antenna measurements is as depicted in **Figure 2**, in which the polar axis is along *z*-axis and antenna axis is aligned along *z*-axis. After this the Ludwig's II definition (transformation) is applied to obtain the co-polar and cross polar patterns. Hence, all the measurements shown in this chapter will be as per L2 definition of cross polarization.

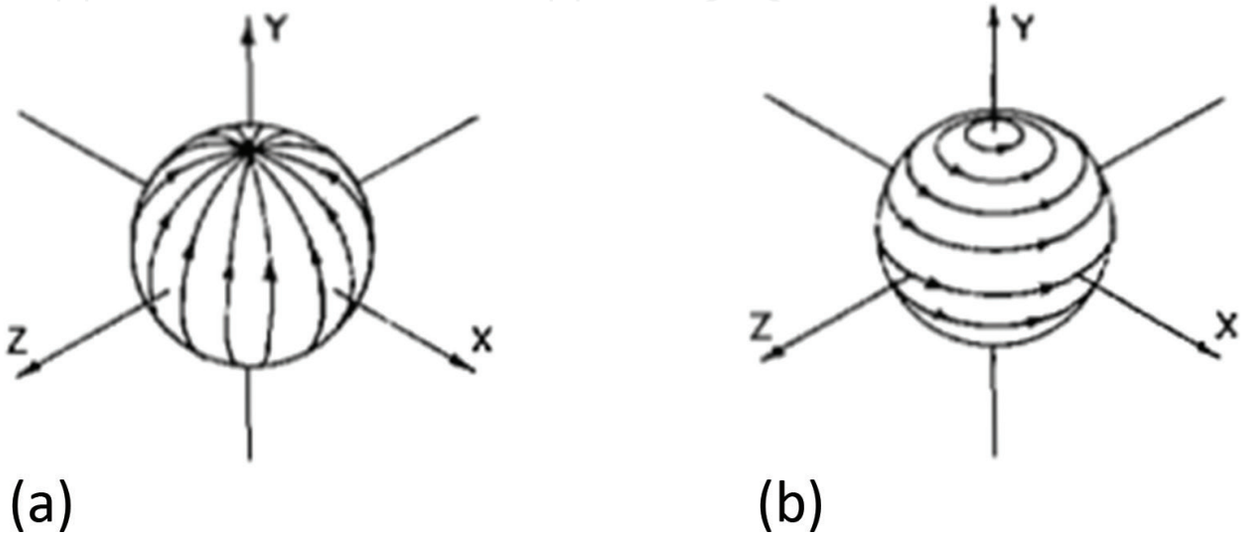

Figure 3. Ludwig II coordinate system [13], (a) direction of reference polarization and (b) direction of cross polarization.

3. Loop as a magnetic dipole

Loop antennas are one of the simple, versatile, and inexpensive forms of microstrip antenna. In this section, the basic condition for a loop to exhibit magnetic dipole characteristics is discussed. The different implementations of loop antennas in order to achieve its requirements are tested. It will be shown that a loop antenna with capacitive loading has uniform current distributions and its simulation results are discussed.

3.1. Magnetic fields due to constant current loop

The loop antenna can behave as magnetic dipole when it has constant current along its circumference. To illustrate this, consider a loop with constant current i, radius r, and an observation point at a far-field distance R as shown in **Figure 4**. At far-field distance where ($R \gg r$), the loop can be treated as a small circular loop with constant current, and the calculation of magnetic field depends on the current i, R, and θ, i.e., the angle form the z-axis. The magnetic field equations are given by [14]

$$B = \begin{cases} B_r = 2|\mu|\mu_0 \frac{cos\theta}{4\pi R^3} \\ B_\theta = |\mu|\mu_0 \frac{sin\theta}{4\pi R^3} \end{cases} \tag{3}$$

Where $\mu = iA$ is the magnetic dipole moment of the loop and A is the area of the loop. These magnetic fields produced by the loop are equivalent to the fields produced by a small magnetic dipole. The magnetic dipole moment as stated above is a vector pointing out normal to the plane of the loop, and its magnitude is equal to the product of current and area of the loop.

3.2. Design and simulation results of loop based on capacitive loading

As aforementioned in Section 3.1, the loop antenna can have the same characteristics like a magnetic dipole if constant unidirectional current is maintained along its circumference.

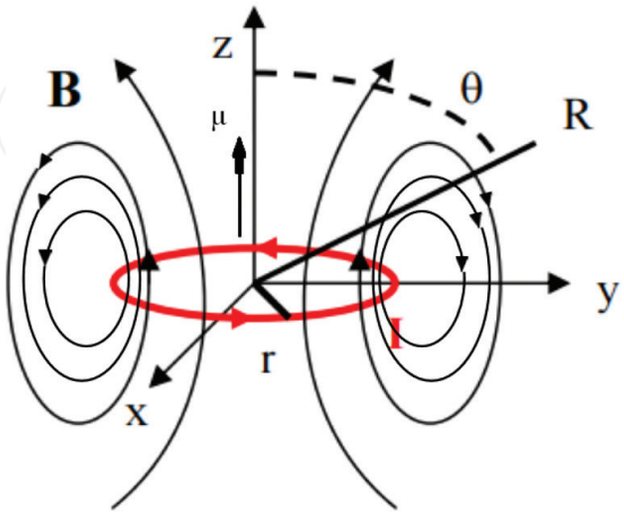

Figure 4. Illustration of magnetic fields around a loop.

http://dx.doi.org/10.5772/66502

This is generally difficult to achieve for smaller loop antennas because of high reactance and small radiation resistance which leads to improper matching [9, 15]. To combat this problem, Foster [16] derived the idea of driving the loop currents in segments which also explains the analytical solution for radiation resistance and directivity for these types of loops. Later Li et al. [17] proved that by adding a capacitive reactance on the loop at every 45°, a uniform traveling wave current distribution can be obtained. A similar concept was used by Wei et al. [18] for designing a horizontally polarized loop antenna. The loop antenna shown in **Figure 5** is reproduced using the original design by Wei et al. [18] with different substrate material and different operating frequencies.

This proposed loop shown in **Figure 5** has periodic capacitive loading at every 45° and consists of strip-line sections which are similar to unit cell described by Park et al. [19]. This unit cell which is periodically placed helps to maintain uniform in-phase surface current distribution on the surface of the loop as seen in **Figure 5(b)** by creating a series capacitance. Therefore, this antenna can meet the condition of behaving as a magnetic dipole in far field.

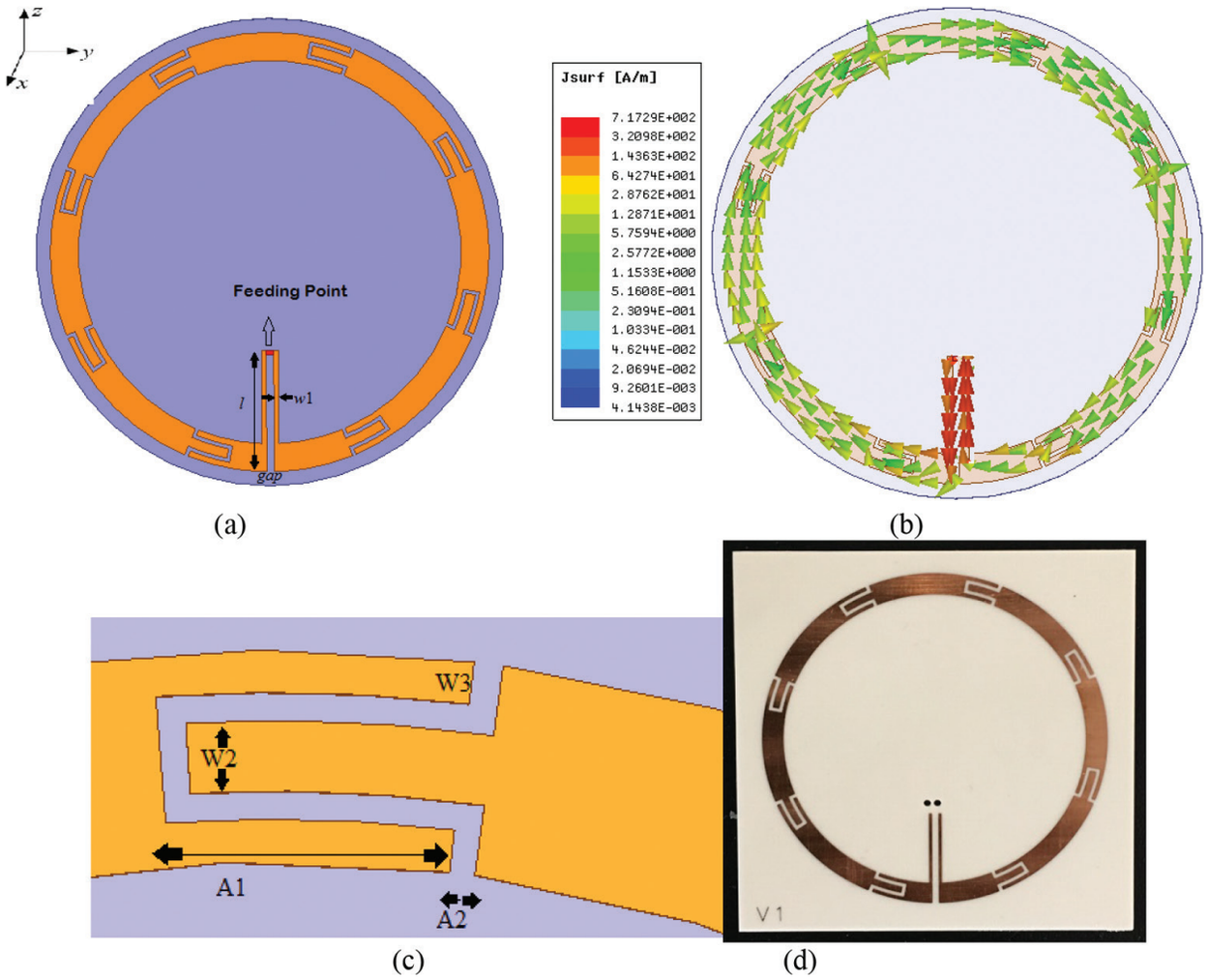

Figure 5. Loop with capacitive loading: (a) design in HFSS, (b) illustration of surface current, (c) dimensions of the unit cell, and (d) fabricated prototype.

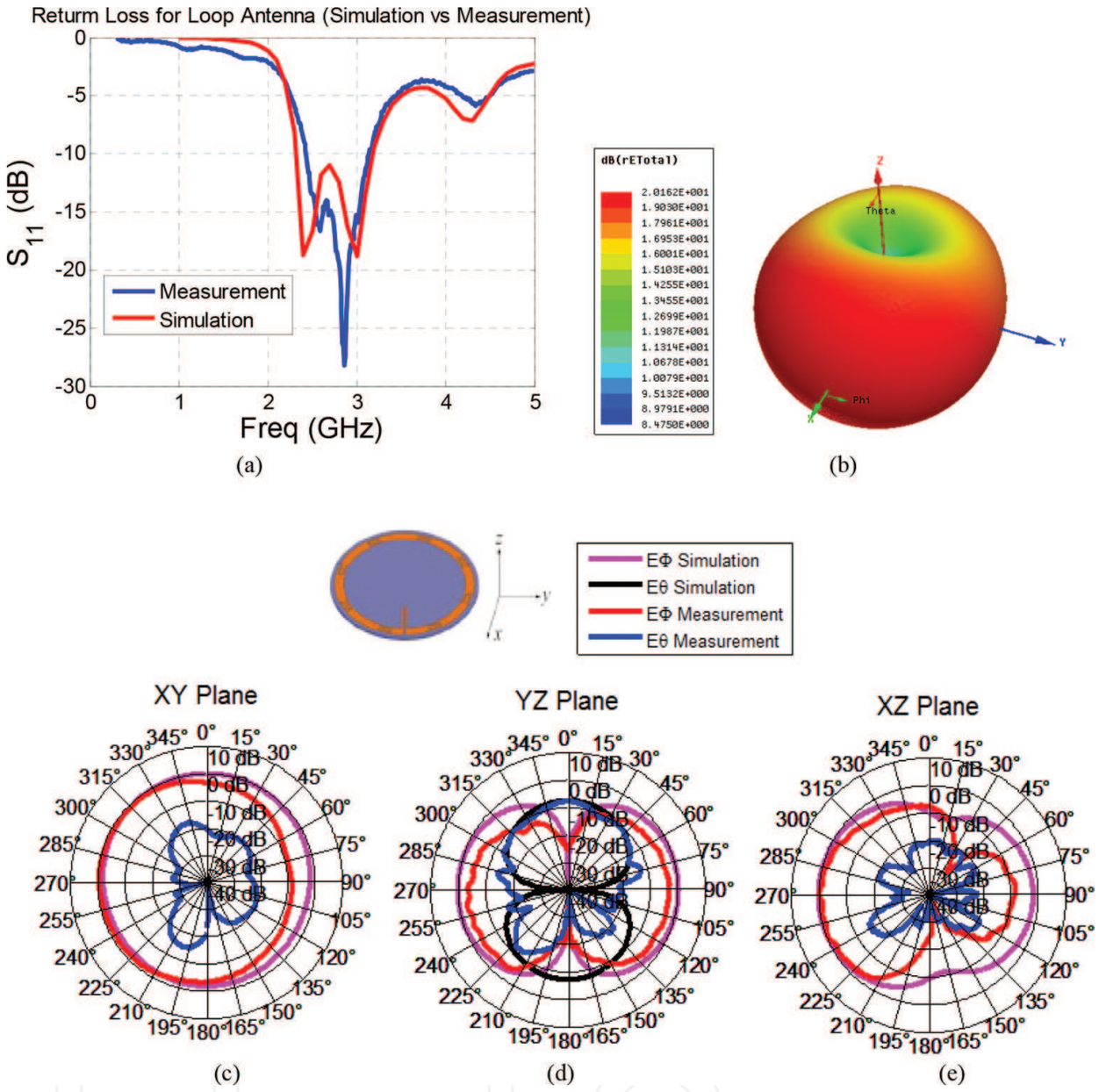

Figure 6. Comparison of measured and simulated pattern: (a) return loss (S_{11}) in dB, (b) total 3D radiation pattern, (c) XY plane cut of the radiation pattern, (d) YZ plane cut of the radiation pattern, and (e) XZ plane cut of the radiation pattern.

The loop is designed on Rogers 4725JXR substrate ($\varepsilon_r = 2.64$) with 0.787 mm thickness with 1 oz. copper. The loop has inner radius (R2) = 20.5 mm and outer radius (R1) = 23.5 mm. Each unit cell of strip line has the following dimensions as depicted in **Figure 5(c)** as $A_1 = 11°$ or 4 mm, $A_2 = 1°$ or 0.35 mm, $w_2 = 1$ mm, and $w_3 = 0.6$ mm. The periodic unit strip-line sections (unit cells) are placed at every 45°. The number of unit cells for capacitive loading are related by relation $A_1 + A_2 = \frac{360}{N}$, where N being the number of unit cells. Another advantage of using the periodic capacitive loading is to achieve a wide impedance bandwidth [18]. The antenna is fed by using a parallel strip-line which is a balanced structure and also plays a role of a balun and helps in maintaining impedance matching. Each strip line has a length (l) = 13 mm,

width (w_1) = 0.5 mm, and gap = 0.8 mm as seen in **Figure 5(a)**. The structure was simulated in Ansoft HFSS simulation software. The absorbing boundary conditions (ABCs) were used in the simulation environment, and the antenna is excited by using lumped port excitation. The ABC boundaries are placed at a distance more than $\frac{\lambda}{4}$ from the antenna.

The SMP connector at the feeding point for the fabricated prototype is shown in **Figure 5(d)**. The return loss (S_{11}) is measured using the PNA and can be seen in **Figure 6(a)**. The antenna is designed to operate over 2.3–3.1 GHz in simulation. However the measured results show that antenna has good return loss over 2.5–3.0 GHz which gives us at least about 500 MHz of bandwidth.

The antenna was simulated at 2.8 GHz and the simulation and measurement results for principal planes are shown in **Figure 6**. As the loop is horizontally polarized, it radiates horizontally polarized fields (E_ϕ, i.e., co-polar radiation for this case). There are also vertically polarized fields (E_θ, i.e., the cross polar radiation for this case) which are unwanted electric fields (orthogonal to desired direction) from the loop. These vertically polarized fields usually exist in the real world due to feeding point variations and material imperfections. It can be observed that the radiation fields of the loop are close to an ideal magnetic dipole as it exhibits a pattern similar to that of a doughnut shape with a null along its axis (in elevation plane) and has maximum radiation along the plane of the loop (XY plane). Ideally, the radiation in XZ plane and YZ plane should be similar for a magnetic dipole; however, because of the feed line design of this loop, there is some electric field radiation from this feed line (two parallel strip lines). This adds up to the cross polar fields and constitutes stronger E_θ in YZ plane.

4. Printed electric dipole

An electric dipole antenna is widely used for many applications and is considered as one of the simplest form of linear wire antennas [20]. The design of a regular linear wire dipole is simple. It consists of a conductor (wire) which is split in the middle to allow the feeder to transmit or receive power.

As shown in **Figure 7**, a dipole consists of two poles; the length of each pole is quarter wavelength ($\frac{\lambda}{4}$), thereby making overall dipole as half-wavelength ($\frac{\lambda}{2}$). The dipole radiates equal power in all azimuthal directions perpendicular to the axis of the antenna. Section 4.1 describes the design and simulation of the dipole used in for this research.

4.1. Design and simulation results of a printed electric dipole

Several types of dipoles are available such as wire dipole, folded dipole, printed dipole, cage dipole, and bow tie and batwing antenna [20]. These are specific to the type of application and decisions of design. In this chapter, the printed dipole is chosen among different variations of dipole antennas, because it is easy to design and does not involve 3D structures. The advantage of light weight, small size, and planar form of dipole can be realized when it is aligned with loop which will be discussed in the next section.

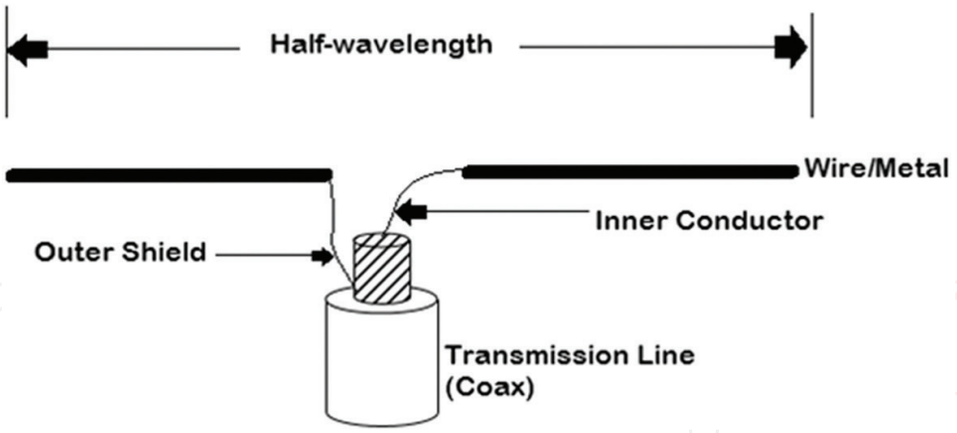

Figure 7. A simple linear wire dipole antenna.

The proposed design is a very simple planar printed electric dipole. This microstrip dipole antenna has two arms or poles as shown in **Figure 8**. Each of the arms has length *L* and width *W* and is separated by a gap *Gap*.

The microstrip printed dipole is designed on Rogers 4725JXR ($\varepsilon_r = 2.64$) with 0.787 mm thickness and 1 oz. copper. The design is based on the equations given below [21]:

$$\varepsilon_e = \frac{\varepsilon_r + 1}{2} + \frac{\varepsilon_r - 1}{2}\left[\frac{1}{\sqrt{1 + 12d/W}}\right] \tag{4}$$

where ε_r = dielectric constant; ε_e = effective dielectric constant; d = substrate thickness; W = width of microstrip line.

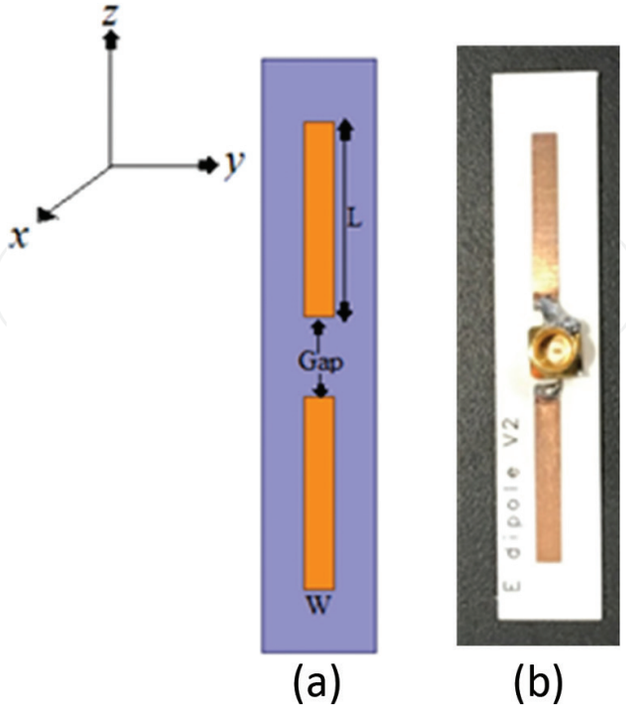

Figure 8. A printed dipole: (a) design and HFSS model and (b) fabricated prototype.

http://dx.doi.org/10.5772/66502

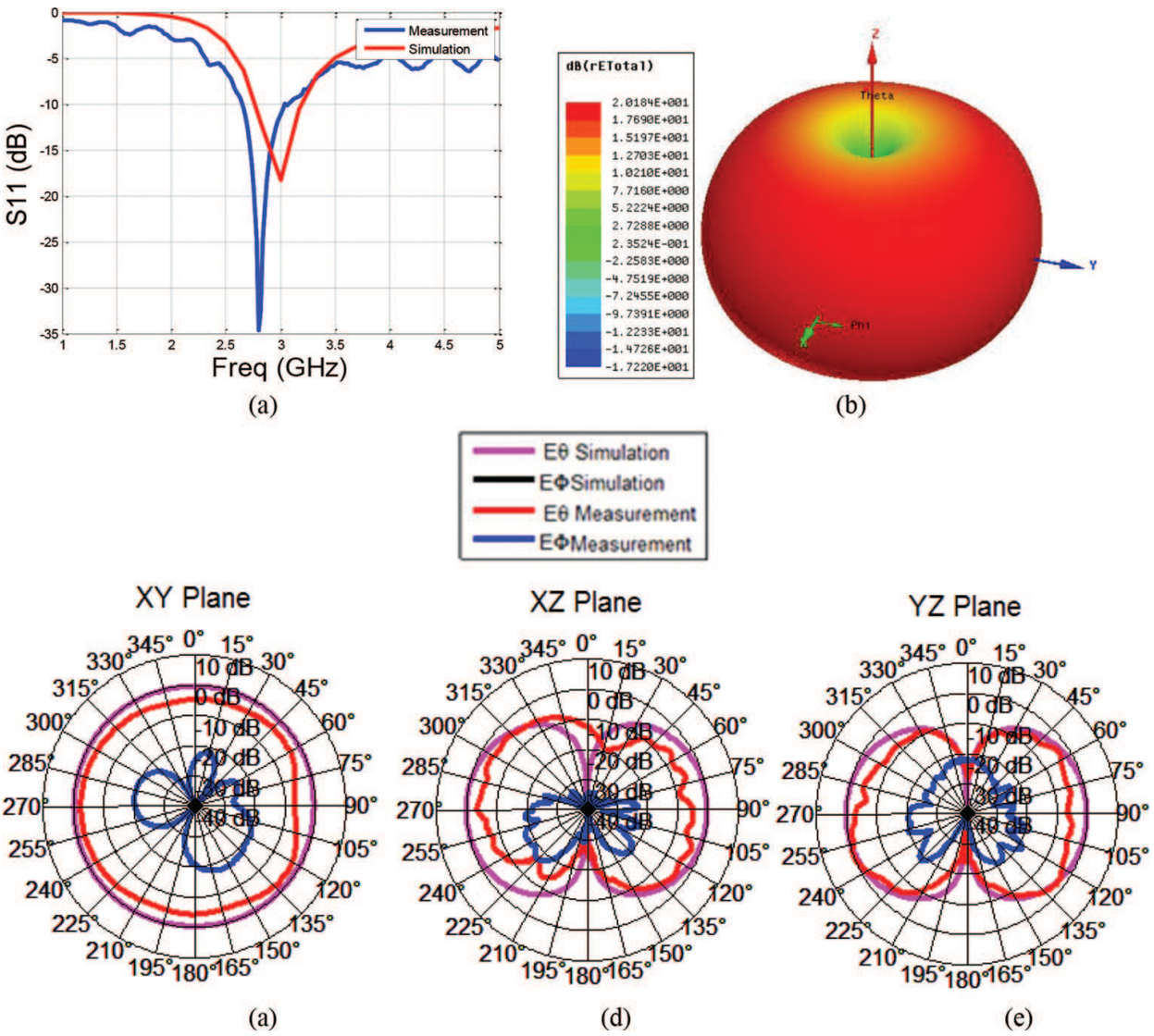

Figure 9. HFSS simulated return loss and radiation patterns of the proposed electric dipole antenna: (a) return loss (S_{11}) in dB, (b) total 3D radiation pattern, (c) XY plane cut of the radiation pattern, (d) XZ plane cut of radiation pattern, and (e) YZ plane cut of radiation pattern..

The length L of the printed dipole is approximated to quarter wavelength ($\frac{\lambda}{4}$) and the entire dipole constitutes half wavelengths ($\frac{\lambda}{2}$). The value "λ" is given by

$$\lambda = \frac{c}{f\sqrt{\varepsilon_e}} \tag{5}$$

where λ = wavelength; c = velocity of light; f = frequency.

These values are tuned and approximated by using the parametric setup in HFSS simulation software. The values used for the above fabricated prototype are $L = 17$ mm, $W = 2.5$ mm, and $Gap = 7$ mm. The antenna is excited by lumped port excitation in HFSS and absorbing boundary conditions (ABCs) was used in the simulation environment. The ABC boundaries are placed at a distance more than $\frac{\lambda}{4}$ from the antenna.

The microstrip electric dipole is operating over 400 MHz bandwidth ranging from 2.7 to 3.1 GHz.

It is seen in **Figure 9(a)** that there is a slight shift in frequency in measured results as compared to simulation. This might be due to the effect of use of SMP connector as shown in **Figure 8(b)** practically, versus an ideal 50 Ω matched lumped port in simulation. The simulation results show the radiation patterns at 2.8 GHz (selected for the convenience of comparing them with measurement results of electric dipole and loop) for principal planes seen in **Figure 9**. Although the electric dipole is designed to radiate vertically polarized fields (E_θ, i.e., the co-polar radiation for this case), it is observed that there are also horizontally polarized fields (E_ϕ, i.e., the cross polar radiation) radiated from the antenna. This cross polar radiation might be due to the factors like antenna aperture, radiation of electric field in unwanted direction (orthogonal to desired direction), material imperfections, and radiation from the feed point. The simulation results show that the plane of maximum radiation is in XY plane, and there is a null along z-axis which is part of the doughnut shape as seen in **Figure 9(b)**.

5. Dual-polarized radiating element

By discussing the design of loop antenna in the previous section, it is clear that the loop antenna has capability to radiated fields which are similar to that of a magnetic dipole. The proposed design of the loop as in Section 3 is an electrically large loop as the circumference of loop is greater than one-tenth of wavelength ($\lambda/10$). But at a far-field distance from the source ($R \gg r$), where R is the observation point and r is the radius of the loop, the loop can be considered as an electrically small loop. This electrically small loop antenna acts as a dual antenna to a short dipole antenna. The far-field electric and magnetic fields of magnetic dipole (loop) are identical to the far-field magnetic and electric field of electric dipole, respectively [22]. This can be illustrated in **Figure 10** [22].

Consider a loop having a uniform current I_0' and area $\Delta S'$. The far-field vector potential for electrically small loop is given by [9, 22] as

$$A \approx j\frac{k\mu I_0 \Delta S}{4\pi r} e^{-jkr} \sin\theta \; a_\phi \tag{6}$$

where $\Delta S = \Delta l^2$, i.e., the area of the loop and a_ϕ is the spherical coordinated vector given by $a_\phi = (-\sin\phi\, a_x + \cos\phi\, a_y)$.

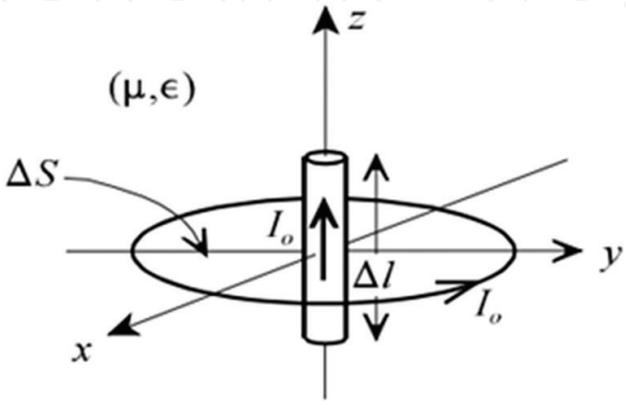

Figure 10. Illustration of collocated loop and electric dipole arrangement [22].

http://dx.doi.org/10.5772/66502

The corresponding far-field components for electrically small loops can be calculated using Eq. (6) as [9, 22]

$$E_{\phi} \approx -j\omega A_{\phi} \approx \frac{\eta k^2 I_0 \Delta S}{4\pi r} e^{-jkr} \sin\theta \tag{7}$$

$$H_{\theta} \approx j\frac{\omega}{\eta} A_{\phi} \approx -\frac{k^2 I_0 \Delta S}{4\pi r} e^{-jkr} \sin\theta \tag{8}$$

If carefully observed, these components are similar to the fields those radiated by an infinitesimal electric dipole [9, 22]. **Table 2** shows the comparison between these two antennas:

Infinitesimal electric dipole	Electrically small loop
$E_{\theta} \approx j\frac{\eta k I_0 \Delta l}{4\pi r} e^{-jkr} \sin\theta$	$E_{\phi} \approx \frac{\eta k^2 I_0 \Delta S}{4\pi r} e^{-jkr} \sin\theta$
$H_{\phi} \approx j\frac{k I_0 \Delta l}{4\pi r} e^{-jkr} \sin\theta$	$H_{\theta} \approx -\frac{k^2 I_0 \Delta S}{4\pi r} e^{-jkr} \sin\theta$

Table 2. Comparison of far-field elements generated by small electric dipoles and loops.

These equations in **Table 2** show that they share the same mathematical form, and a pair of equivalent and dual source can be found out by changing the symbols. This is known as duality theorem [9]. By duality theorem we have dual quantities of electric and magnetic current sources as shown in **Table 3**.

Now by applying the above dual quantities, the far-field components of the magnetic sources can be determined and are shown in **Table 4**.

Therefore, if an electrically small magnetic loop and an electric dipole are designed such that

$$I_o \Delta l = j\eta k I_{om} \Delta S = j\omega\mu I_{om} \Delta S \tag{9}$$

then due to this equivalence condition, the far fields radiated by the electrically small magnetic loop and electric dipole are equivalent dual sources. Since these antennas act as dual to each other, the power radiated by both should be the same when currents and dimensions are appropriately designed.

Electric source	Magnetic source
E	H
H	$-E$
I_o	I_{om}
K	k
H	$\frac{1}{\eta}$

Table 3. Dual quantities for electric and magnetic current sources.

Infinitesimal magnetic dipole	Electrically small loop (magnetic)
$H_\theta \approx j\frac{kI_{0m}\Delta l}{\eta 4\pi r}e^{-jkr}\sin\theta$	$H_\phi \approx \frac{k^2 I_{0m}\Delta S}{\eta 4\pi r}e^{-jkr}\sin\theta$
$E_\phi \approx -j\frac{kI_{0m}\Delta l}{\eta 4\pi r}e^{-jkr}\sin\theta$	$E_\theta \approx \frac{k^2 I_{0m}\Delta S}{\eta 4\pi r}e^{-jkr}\sin\theta$

Table 4. Far-field components of corresponding magnetic sources.

5.1. Antenna arrangement and polarization

From the above discussion, it is lucrative to determine the antenna configuration/alignment which will be useful to form a dual-polarized antenna unit. In theory, an electric dipole and electrically small loop (magnetic dipole) are dual antennas to each other; their far fields are orthogonal to each other if these antennas are aligned as shown in **Figure 11**. A combination of E&M dipoles is oriented such that the electric field of electric dipole (E_θ) is orthogonal to the electric field of the loop (E_ϕ) everywhere. In other words it can be said as electric dipole should be vertically polarized and loop should be horizontally polarized as shown in **Figure 11(a)**. This can also be illustrated by considering a sphere consisting of latitudes and longitudes. The directions of the fields generated by a loop (magnetic dipole) can be approximated by latitude lines, whereas the direction of the fields generated by electric dipole can be approximated by longitude lines (**Figure 11(b)**). The plane of maximum radiation for the loop and the electric dipole is XY plane. The electric dipole generates quasi vertically polarized waves (i.e., E_θ), and the horizontally polarized loop generates quasi horizontally polarized waves (i.e., E_ϕ).

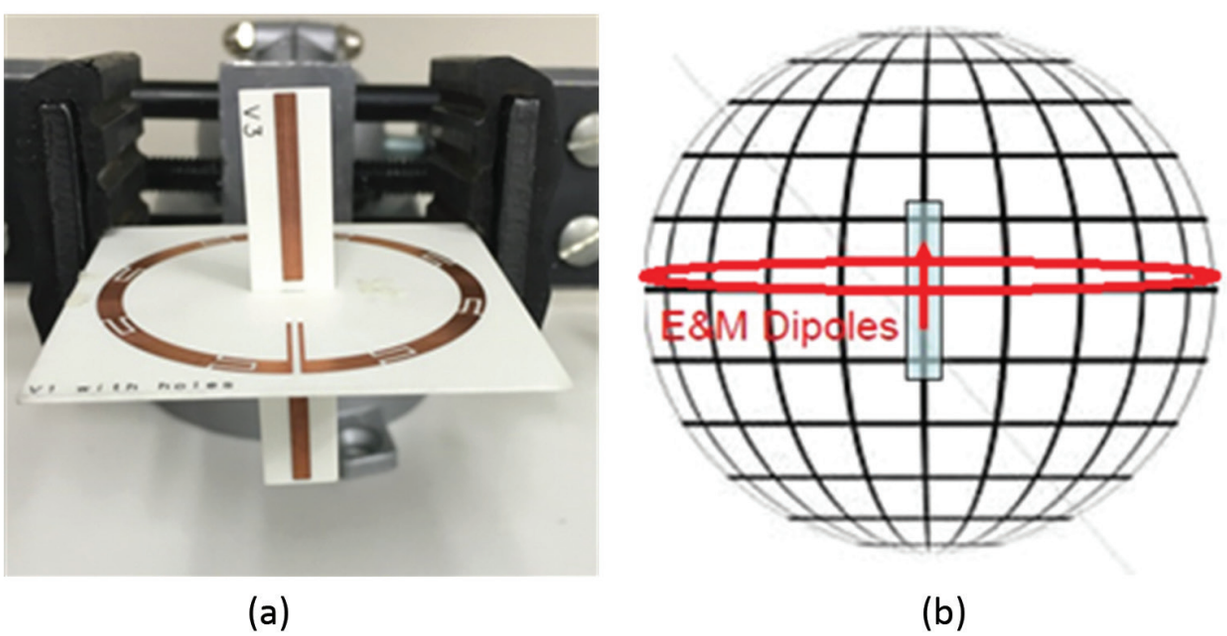

Figure 11. E&M dipole configuration: (a) collocated arrangement and (b) electric field lines due to collinear arrangement of E&M dipoles.

http://dx.doi.org/10.5772/66502

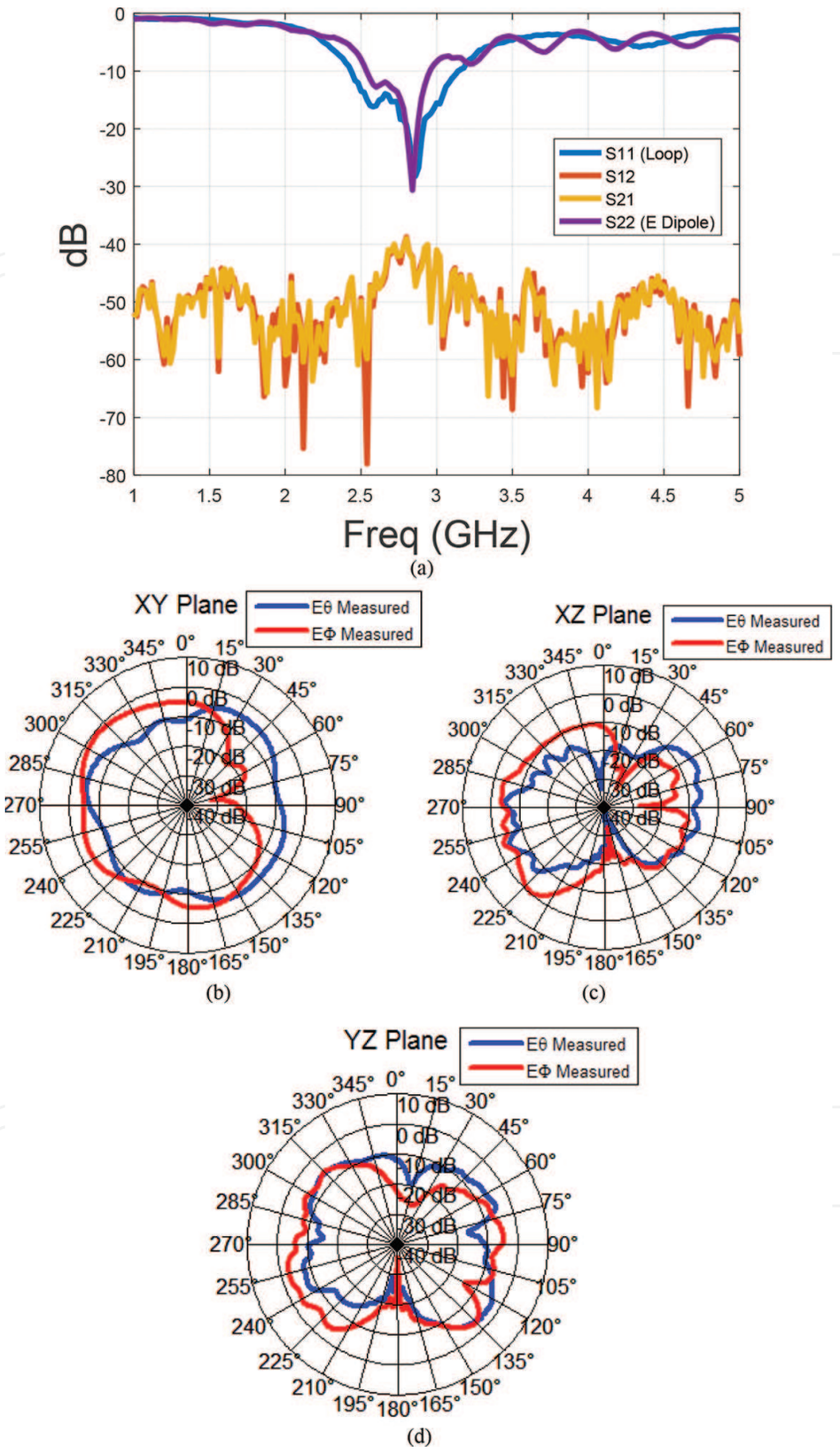

Figure 12. Measurement results when the E dipole antenna and loop antenna are excited simultaneously: (a) measured S-parameters (dB), (b) XY plane cut of the radiation pattern, (c) XZ plane cut of the radiation pattern, and (d) YZ plane cut of the radiation pattern.

This arrangement of electric dipole and loop antenna as discussed above is studied in HFSS simulation, and a fabricated prototype is built as seen in **Figure 11(a)** to measure them in anechoic chambers. The measured S-parameters seen in **Figure 12(a)** show that both electric and magnetic dipoles resonate at 2.8 GHz and have good isolation of about 40 dB in the impedance bandwidth. The measured radiation pattern is illustrated in **Figure 12** for principal planes when both E&M dipoles are excited simultaneously (i.e., H and V simultaneous transmission). The results show that the radiation patterns of both the antennas match very well and these are dual antenna to themselves. The loop generates horizontally polarized waves, and electric dipole generates vertically polarized waves which are orthogonal to each other, thereby serving to be a good candidate for phased array antenna element.

6. E&M dipole array

An array can be built based on the proposed collocated E&M dipole units to emulate a linear subarray for future Multi-functional Phased Array Radar (MPAR). An array can be formed by placing each E&M dipole unit about half wavelengths ($\frac{\lambda}{2}$) from center to center. An investigation of using these elements in a linear form of array is being carried out. The following **Figure 13** shows a simple arrangement of such eight collocated E&M dipole units.

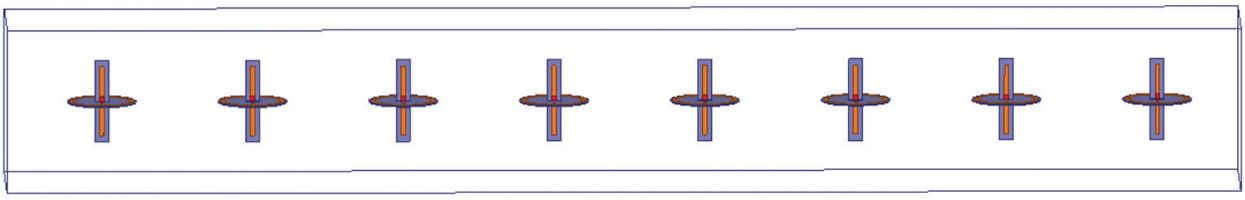

(a)

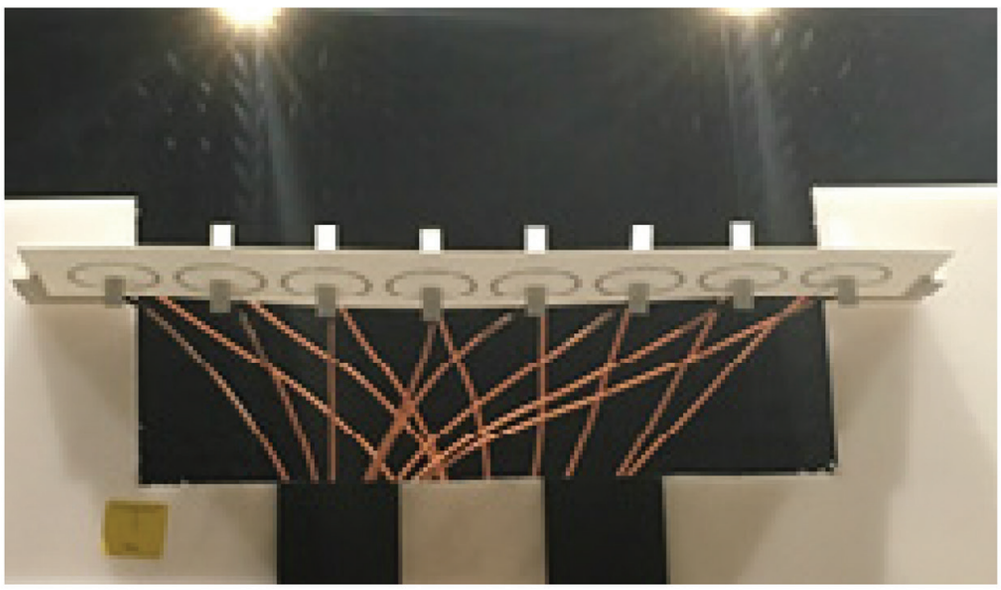

(b)

Figure 13. An eight-element E&M dipole array: (a) simulation using HFSS and (b) fabricated prototype and its measurement setup in anechoic chambers.

http://dx.doi.org/10.5772/66502

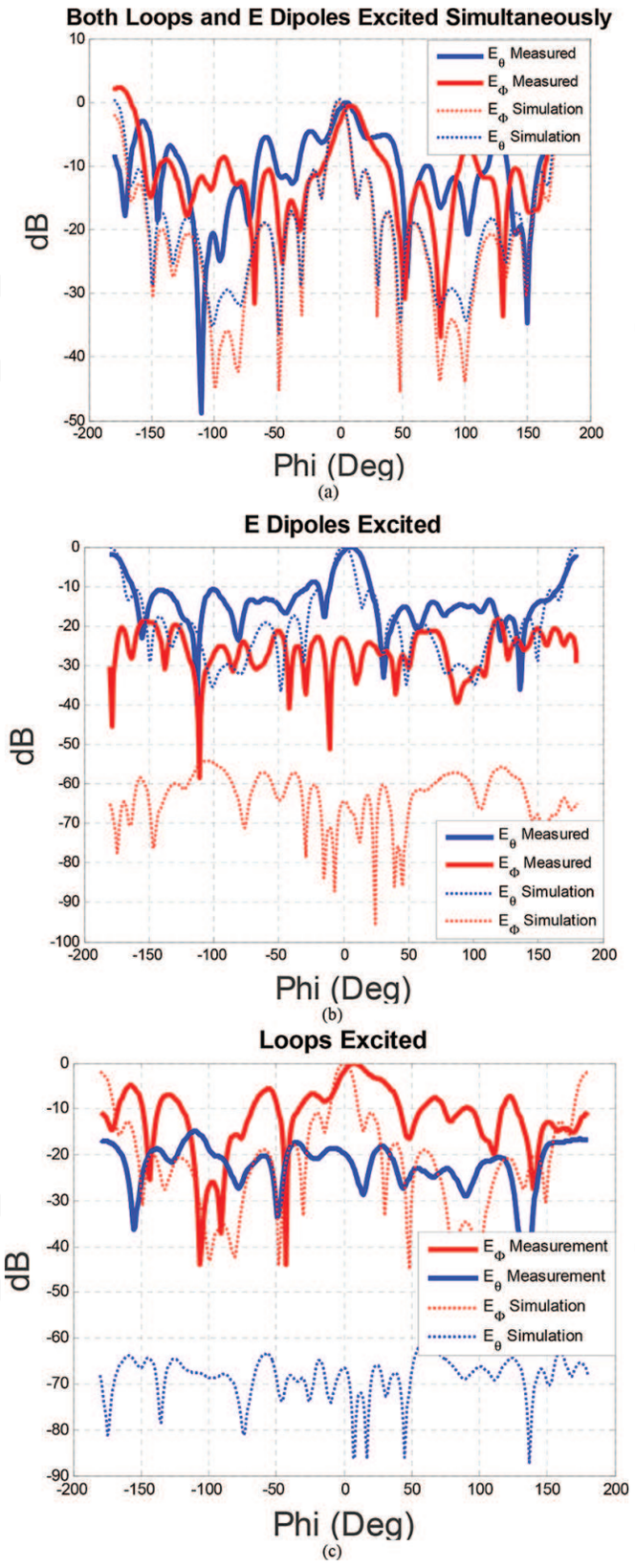

Figure 14. Illustration of co-polar and cross polar fields (amplitudes in dB) for simulation and measurement when (a) both E&M elements are excited in the array, (b) only magnetic loops are excited, and (c) only E dipoles are excited.

If each of these eight collocated units (16 elements) are excited with equal phase and equal amplitude, then it can be seen in **Figure 14(a)** that copolar H and V fields match exactly to each other which meets the requirement for weather applications (proves to be effective in extracting more hydrological parameters) and gives better resolution of the target [2]. On the other hand, if only magnetic loop is transmitting and E dipole is receiving or vice versa, the cross polar radiation is observed to be more than 70 dB lower than the peak co-polar field. These results are illustrated in **Figure 14**.

The simulation results shown above in **Figures 13** and **14** are based on the ideal environment which might differ in the case of practical construction of an array structure. The practical structure of array has feed lines, large backplane (aluminum), support structure for electronics, and other practical factors which might affect the array performance. This can actually have an adverse effect on the cross polarization levels of the array, and it is because of this we see that the simulation and measurement results of the array differ. Due to this reason, we see that the measurement results shown in **Figure 14** differ slightly from simulation. The measurement process involves extensive measures taken to achieve the best possible results, but the interferences from the feed lines and mounting structures are evident. The measurement results shown in **Figure 14** are for uncalibrated array without using any type of phase shifters for beam forming. In addition, the limitations such as availability of ideal probes which have purer linear polarization than AUT make the suppression of cross polarization more difficult.

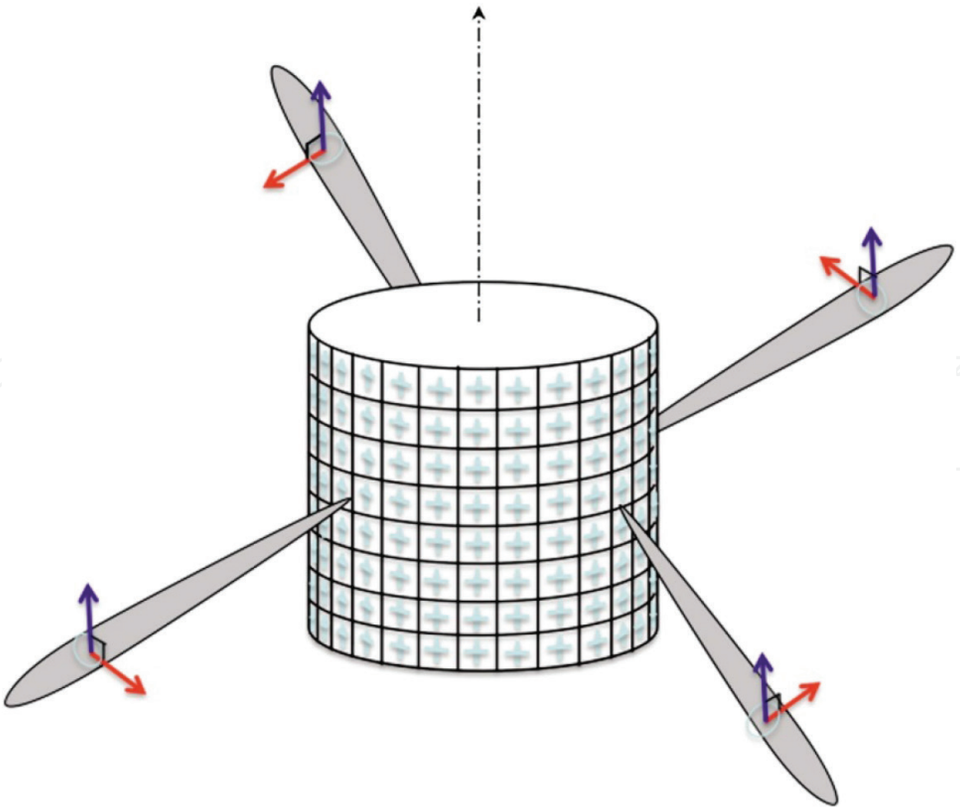

Figure 15. CPPAR with a pair of dipoles for each array element [8].

http://dx.doi.org/10.5772/66502

The concept of E&M dipole cannot only be implemented in linear arrays, but also extended for a cylindrical polarimetric phased array radar (CPPAR) as demonstrated in **Figure 15**. The use of CPPAR has its own advantages like scan invariant polarization basis and low sensitivity loss [8]. In addition to this, the use of the dipole elements can avoid surface waves and creeping waves. However, this is at the cost of more complex and expensive fabrication process. As aforementioned, this study is a step toward designing a new type of dual-polarized array elements based on EM dipole concept on which future research can be conducted. Initial array fabrication and testing are to be performed in a larger array test-bed called Configurable Phased Array Demonstrator (CPAD) at the Radar Innovations Laboratory (RIL), University of Oklahoma.

7. Conclusion

A dual-polarized radiating element for MPAR is proposed by using two simple types of microstrip radiating elements. As aforementioned, this work is a step toward designing and realizing a dual-polarized array element based on electromagnetic dipole concept. The intention of this chapter is to demonstrate a possible new design and build a foundation on which future research can be conducted.

This chapter shows the investigation for two different types of elements which can be collocated to form a dual-polarized element for phased array radars. The array element is a fundamental building block for an array antenna, and it is required that these elements have high cross polarization suppression capacity. The electric dipole takes the form of printed dipole. The magnetic dipole is realized by a simple loop with capacitive loading which maintains uniform surface current. An ideal electric dipole should produce only vertically polarized waves (i.e., E_{θ}), whereas an ideal magnetic dipole should generate only horizontally polarized waves (i.e., E_{ϕ}) which is free of any cross polar radiation. Nevertheless, these elements when realized practically have secondary cross polar fields due to practical factors in design and assembly and radiation from feed lines. For weather polarimetry it is expected that the elements maintain cross polarization factor of about 40 dB for simultaneous transmit/receive and 20 dB for alternate transmit/receive [6]. However, these numbers are for the array level design, but we expect that if the cross polarization isolation is minimized at the element level, then it is expected that with array level implementation, one can achieve this goal.

The measurement process involves extensive measures taken to achieve the best possible results, but the interferences from the feed lines and mounting structures are evident. The measurements performed in the anechoic chambers show the cross polarization of these elements to be about 20 dB lower than peak co-polar field. In addition, the limitations such as availability of ideal probes which have purer linear polarization than AUT make the suppression of cross polarization more difficult.

There are few aspects in which the current design of the elements can be improved. One significant improvement can be a design of a proper feed line using techniques such as proximity feed, aperture coupled feed, etc. This feeding design can be carried forward and improved by

also considering the mechanical design and ease of feeding these elements when assembled into an array. It would be lucrative to see a linear array constructed using these elements such that the cross polar fields are further reduced.

Acknowledgements

Parts of this chapter are reproduced from the MS Degree Dissertation of the first author. This work is supported by NOAA-NSSL through grant #NA11OAR4320072. Any opinions, findings, conclusions, or recommendations expressed in this publication are those of the authors and do not necessarily reflect the views of the National Oceanic and Atmospheric Administration.

Author details

Ridhwan Khalid Mirza[1], Yan (Rockee) Zhang[1]*, Dusan Zrnic[2] and Richard Doviak[2]

*Address all correspondence to: rockee@ou.edu

1 Intelligent Aerospace Radar Team, Advanced Radar Research Center, School of ECE, University of Oklahoma, Norman, USA

2 National Severe Storm Laboratory, NOAA, Oklahoma, Norman, USA

References

[1] NOAA National Severe Storms Laboratory [Online]. Available: http://www.nssl.noaa.gov/tools/radar/mpar/, 2016, 20th January 2016.

[2] D. S. Zrnic, V. M. Melnidov, and R. J. Doviak, "*Issues and challenges for polarimetric measurement of weather with an agile beam phased array radar*," NOAA/NSSL report, [Updated: 2 May 2013], 2013.

[3] C. E. Baum, "Symmetry in electromagnetic scattering as a target discriminant," in *Optical Science, Engineering and Instrumentation'97*, 1997, pp. 295-307.

[4] D. Vollbracht, "Understanding and optimizing microstrip patch antenna cross polarization radiation on element level for demanding phased array antennas in weather radar applications," *Advances in Radio Science,* vol. 13, pp. 251-268, 2015.

[5] Kuloglu, Mustafa. "Development of a Novel Wideband Horn Antenna Polarizer and Fully Polarimetric Radar Cross Section Measurement Reference Target." PhD diss., The Ohio State University, 2012. [Web]. Available:https://etd.ohiolink.edu/rws_etd/document/get/osu1338387100/inline

[6] Y. Wang and V. Chandrasekar, "Polarization isolation requirements for linear dual-polarization weather radar in simultaneous transmission mode of operation," *Geoscience and Remote Sensing, IEEE Transactions on*, vol. 44, pp. 2019-2028, 2006.

[7] F. Mastrangeli, G. Valerio, A. Galli, A. De Luca, and M. Teglia, "An attractive S-band dual-pol printed antenna for multifunction phased array radars," in *Antennas and Propagation (EUCAP), Proceedings of the 5th European Conference on*, pp. 514-516, 2011.

[8] G. Zhang, R. J. Doviak, D. S. Zrnic, R. Palmer, L. Lei, and Y. Al-Rashid, "Polarimetric phased-array radar for weather measurement: a planar or cylindrical configuration?," *Journal of Atmospheric and Oceanic Technology*, vol. 28, pp. 63-73, 2011.

[9] C. A. Balanis, *Antenna theory: analysis and design* vol. 1: John Wiley & Sons, 2005.

[10] W. J. Wu, R. Fan, Z. Y. Zhang, W. Zhang, and Q. Zhang, "A shorted dual-polarized cross bowtie dipole antenna for mobile communication Systems," in *General Assembly and Scientific Symposium (URSI GASS), 2014 XXXIth URSI*, pp. 1-4, 2014.

[11] K. M. Mak, H. Wong, and K. M. Luk, "A shorted bowtie patch antenna with a cross dipole for dual polarization," *IEEE Antennas and Wireless Propagation Letters,* vol. 6, pp. 126-129, 2007.

[12] Y. Liu, H. Yi, F. W. Wang, and S. X. Gong, "A novel miniaturized broadband dual-polarized dipole antenna for base station," *IEEE Antennas and Wireless Propagation Letters*, vol. 12, pp. 1335-1338, 2013.

[13] A. Ludwig, "The definition of cross polarization," *Antennas and Propagation, IEEE Transactions on*, vol. 21, pp. 116-119, 1973.

[14] D. Acosta. *Enriched Physics 2 Lecture* [Web]. Available: http://www.phys.ufl.edu/~acosta/phy2061/lectures/MagneticDipoles.pdf, 2016, 23rd February

[15] J. D. Kraus, Antennas, Tata McGraw Hill Edition,1988. [Web]. Available:http://117.55.241.6/library/E-Books/Antennas_mcgraw-hill_2nd_ed_1988-john_d_kraus.pdf.

[16] D. Foster, "Loop antennas with uniform current," *Proceedings of the IRE,* vol. 32, pp. 603-607, 1944.

[17] R. Li, N. Bushyager, J. Laskar, and M. Tentzeris, "Circular loop antennas reactively loaded for a uniform traveling-wave current distribution," in *Antennas and Propagation Society International Symposium, 2005 IEEE*, pp. 455-458, 2005.

[18] K. Wei, Z. Zhang, and Z. Feng, "Design of a wideband horizontally polarized omnidirectional printed loop antenna," *Antennas and Wireless Propagation Letters, IEEE,* vol. 11, pp. 49-52, 2012.

[19] J. H. Park, Y. H. Ryu, and J. H. Lee, "Mu-zero resonance antenna," *Antennas and Propagation, IEEE Transactions on,* vol. 58, pp. 1865-1875, 2010.

[20] *Dipole Antenna* [Web]. Available: https://en.wikipedia.org/wiki/Dipole_antenna, 2016, 5th March 2016.

[21] D. M. Pozar, *Microwave engineering*: John Wiley & Sons, 2009.

[22] D. J. P. Donohoe. (23 rd February), Mississippi State University. [Web].Available:http://my.ece.msstate.edu/faculty/donohoe/ece4990notes5.pdf

IntechOpen